In-vitro metabolomics to evaluate toxicity of particulate matter under environmentally realistic conditions

Accepted Manuscript

In-vitro metabolomics to evaluate toxicity of particulate matter under environmentally realistic conditions

Francisco Sánchez-Soberón, Matthias Cuykx, Noemi Serra, Victoria Linares, Montserrat Bellés, Adrian Covaci, Marta Schuhmacher

PII: S0045-6535(18)31140-8

DOI: 10.1016/j.chemosphere.2018.06.065

Reference: CHEM 21597

To appear in: *ECSN*

Received Date: 19 March 2018

Revised Date: 7 June 2018

Accepted Date: 8 June 2018

Please cite this article as: Sánchez-Soberón, F., Cuykx, M., Serra, N., Linares, V., Bellés, M., Covaci, A., Schuhmacher, M., *In-vitro* metabolomics to evaluate toxicity of particulate matter under environmentally realistic conditions, *Chemosphere* (2018), doi: 10.1016/j.chemosphere.2018.06.065.

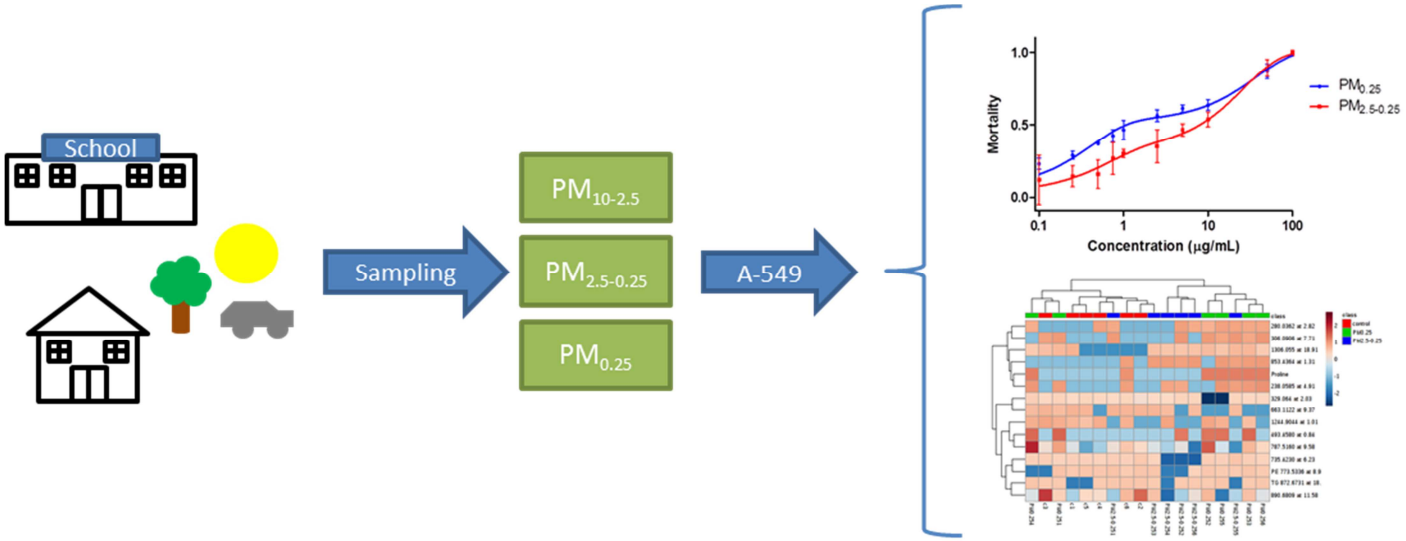

In-vitro metabolomics to evaluate toxicity of particulate matter under environmentally realistic conditions

Francisco Sánchez-Soberón[1], Matthias Cuykx[2], Noemi Serra[3], Victoria Linares[3], Montserrat Bellés[3], Adrian Covaci[2], Marta Schuhmacher[1*]

[1]*Universitat Rovira i Virgili, Chemical Engineering Department, Environmental Analysis and Management Group, Av. Països Catalans 26, 43007 Tarragona, Spain*

[2]*Toxicological Center, Department of Pharmaceutical Sciences, University of Antwerp, Universiteitsplein 1, 2610 Antwerp, Belgium*

[3]*Universtiat Rovira i Virgili, School of Medicine, Laboratory of Toxicology and Environmental Health, San Lorenzo 21, 43201 Reus, Spain*

*Corresponding author: marta.schuhmacher@urv.cat

Declarations of interest: none

[1]

Abbreviations: ACN: Acetonitrile; CCOHS: Canadian Centre for Occupational Health and Safety; CERs: Ceramides; $CHCl_3$: Chloroform; Cho: Choline; CLs: Cardiolipins; Etn: Ethanolamine; EU: European Union; FA: Formic Acid; HAc: Acetic Acid; IC_5: 5% Inhibitory Concentration; IPA: Isopropanol; MeOH: Methanol; NH_4Ac : Ammonium Acetate; NH_4F: Ammonium Formate; LC-MS: Liquid Chromatography-Mass Spectrometry; P: Pulmonary; PBS: Phosphate Buffered Saline; PC: Polycarbonate; PCs: Phosphatidylcholines; PEMT: Phosphatidyl-Ethanolamine N-Methyltransferase; PEs: Phosphatidylethanolamines; PGs: Phosphatidylglycerols; PM: Particulate Matter; PSs: Phosphatidylserines; QC: Quality Control; Ser: Serine; TB: Tracheobronchial; TEHP: 2-ethylhexyl phosphate; TG: Triglycerides; US EPA: United States Environmental Protection Agency; WHO: World Health Organization.

[1]

Keywords

Particulate matter; Indoor sampling; A549; Cytotoxicity; HP-LC/MS; Metabolomics

Abstract

In this pilot study three fractions of particulate matter ($PM_{0.25}$, $PM_{2.5-0.25}$, and $PM_{10-2.5}$) were collected in three environments (classroom, home, and outdoors) in a village located nearby an industrial complex. Time-activity pattern of 20 students attending the classroom was obtained, and the dose of particles reaching the children's lungs under actual environmental conditions (i.e. real dose) was calculated via dosimetry model. The highest PM concentrations were reached in the classroom. Simulations showed that heavy intensity outdoor activities played a major role in PM deposition, especially in the upper part of the respiratory tract. The mass of $PM_{10-2.5}$ reaching the alveoli was minor, while $PM_{2.5-0.25}$ and $PM_{0.25}$ apportion for most of the PM mass retained in the lungs. Consequently, $PM_{2.5-0.25}$ and $PM_{0.25}$ were the only fractions used in two subsequent toxicity assays onto alveolar cells (A549). First, a cytotoxicity dose-response assay was performed, and doses corresponding to 5% mortality (LC_5) were estimated. Afterwards, two LC-MS metabolomic assays were conducted: one applying LC_5, and another applying real dose. A lower estimated LC_5 value was obtained for $PM_{0.25}$ than $PM_{2.5-0.25}$ (8.08 and 73.7 ng/mL respectively). The number of altered features after LC_5 exposure was similar for both fractions (39 and 38 for $PM_{0.25}$ and $PM_{2.5-0.25}$ respectively), while after real dose exposure these numbers differed (10 and 5 for $PM_{0.25}$ and $PM_{2.5-0.25}$ respectively). The most metabolic changes were related to membrane and lung surfactant lipids. This study highlights the capacity of PM to alter metabolic profile of lung cells at conventional environmental levels.

1. Introduction

Particulate matter (PM) is recognized as one of the most harmful air pollutants (Megido et al., 2016). PM consists of liquid droplets and solid fragments smaller than 10 µm suspended in the air,

whose size, chemical composition, and shape are varied (WHO, 2014). For regulatory purposes, environmental agencies all over the world usually classify PM into two groups according to its size: PM_{10} (those particles having a diameter smaller than 10 µm, sometimes named as respirable) and $PM_{2.5}$ (smaller than 2.5 µm, also referred as fine) (European Commission and EU Parliament, 2008; US EPA, 2016). Several studies agree that the smaller the PM, the more harmful it is, since it is usually enriched in toxic components, such as polycyclic aromatic hydrocarbons (PAHs) and heavy metals, and it can reach deeper parts of the respiratory system (Kelly and Fussell, 2016).In fact, it is estimated that $PM_{2.5}$ is responsible of more than 2 million premature deaths per year globally (Donahue et al., 2016).

In vitro tests have been used to assess the toxicity of PM (Wu et al., 2018). The classical approach in these assays consists of applying varying doses of toxicant on different cell types, and study parameters such as cytotoxicity, genotoxicity, strength of cell junction or apoptosis (X. Cao et al., 2015; Chen et al., 2017; Peixoto et al., 2017). Although it is possible to find examples of papers focused on studying the effects of PM under realistic conditions (van Drooge et al., 2017), these studies are conventionally used as a way of studying elicited effects of PM on cells for short term exposures (usually 24 hours) and doses higher than those experienced in environmental conditions.

To have a better approach of observing changes in cells at low and real doses, omics sciences are a powerful tool. Omics are a series of disciplines focused on studying the complete profile of genes (genomics), mRNA (transcriptomics), proteins (proteomics), or metabolites (metabolomics) for a given cell type or organism (Horgan and Kenny, 2011). Although nowadays papers applying different omics methods on lung cells have been published, the number of studies assessing toxicity of ambient PM by omics means is still low (Q. Huang et al., 2015; Líbalová et al., 2012; Longhin et al., 2016; Vaccari et al., 2015; Wang et al., 2017; Wheelock et al., 2013; Zhang et al., 2017). Furthermore, although some papers using omics techniques to evaluate PM toxicity under exposure conditions typical of general population living in western countries can be found (Mesquita et al., 2015), to the best of our knowledge there is no paper assessing such a thing onto pulmonary cells.

The aim of the present study is to have a deeper understanding of health effects on human lung cells when exposed to PM under low dose and mid-term exposure conditions. To do so, three fractions of PM ($PM_{10-2.5}$, $PM_{2.5-0.25,}$ and $PM_{0.25}$) were collected in three different environments (outdoors, inside a classroom, and inside a domestic living room) nearby an industrial area in the Tarragona County (Catalonia, Spain). To calculate the exposure of kids attending the classroom, time-activity pattern of children attending the school was gathered, Subsequently, a dosimetry model (MPPD) was used to calculate real dose of PM reaching the children's lungs. To have an overview of the total toxicity of the PM, a cytotoxicity assay was performed after exposing human alveolar cells (A549) to different doses of those fractions of PM able to reach the lungs (i.e. $PM_{2.5-0.25}$ and $PM_{0.25}$). Finally, to have a better insight of hazardous potential of these materials, a metabolomic assay was performed by exposing the cells at LC_5 (concentration of PM causing a 5% mortality) and a real dose of the two fractions during mid-term (72 h) exposure time.

2. **Methods**

2.1. Materials, chemicals, and standards

Polycarbonate (PC) filters for sampling were purchased from Whatman (Maidstone, UK). Lung carcinoma cells A549 (ATCC® CCL-185™), culture media and supplements, methylthiazolyldiphenyl-tetrazolium bromide (MTT) reagent, and detergent reagent were obtained from ATCC (Teddington, UK). Phosphate buffered saline (PBS), methanol (MeOH), and acetonitrile (ACN) were obtained from Thermo Fisher (Waltham, MA, USA). Chloroform ($CHCl_3$), isopropanol (IPA), ammonium acetate (NH_4Ac), acetic acid (HAc), formic acid (FA), and ammonium formate (NH_4F) were obtained from Merck KGaA (Darmstadt, Germany). Chamber slides, tributylamine (TBA), 2-ethylhexyl phosphate, and succinic acid-d4 were obtained from Sigma-Aldrich (St. Louis, MO, USA). Cholesterol-d4, lauric acid-d3, and tryptophane-d5 were obtained from CDN Isotopes (Pointe-Claire, Quebec, Canada).

2.2. PM sampling and extraction

Samples of $PM_{10-2.5}$, $PM_{2.5-0.25}$ and $PM_{0.25}$ were collected simultaneously from 2nd to 6th of May 2016 in Perafort (Tarragona province, Spain). This location is settled in a suburban area, where the air is influenced by the presence of an industrial estate located 3 km south-west (Figure S1). This industrial area comprises an oil refinery and several chemical companies (MAPAMA, 2018). Samples were collected in three different environments: inside a classroom, inside a living room, and outdoors. These environments were in the same village, within a 200 meters radius. The volume of the classroom was 173.25 m^3, and 20 students were attending the class during sampling. The house living room had 40.43 m^3 and was occupied by three nonsmoking people. Regarding the outdoor sample, it was collected in the first-floor terrace of the same school at which the classroom belongs. No ventilation was registered during the sampling period in the indoor environments. Samples were collected onto (PC) filters using cascade impactors (Siotuas™, SKC Inc. Eighty-Four, PA, USA) connected to a pump (Leland Legacy, SKC). Two samplers were placed in every environment, working simultaneously at a flow rate of 9 L/min. After 48 h, PC filters were replaced, till having a total of 4 samples per fraction and environment. Before and after sampling, filters were weighted several times till reaching a constant weight on a 10-µg accuracy microbalance. Masses of PM were calculated as the differences in filters weight before and after sampling. Particulate matter concentrations in air were then calculated by dividing the masses by the total sampled air volume.

To extract PM from PC filters, these were submerged into tubes containing deionized water, shaken for 20 min and sonicated for 10 min. Subsequently, filters were removed from the tubes, dried at room temperature, and weighted again. The supernatants were centrifuged at 3500 rpm., freeze-dried, and stored at -20 ºC until further analysis. Extraction recoveries for PM ranged between 92 and 102%. Clean PC filters subjected to the same extraction procedure were used as negative control.

2.3. Children activity pattern

To calculate the real dose of PM inhaled by children, physical activities performed in every microenvironment as well as the duration of these activities were registered. 20 nine- to ten-year old students attending the sampling room were asked to describe their daily routine. Their routine was classified into 6 different activities: heavy exercise outdoors, light exercise outdoors, light exercise at home, sitting at school, sitting at home, and sleeping time.

2.4. Calculation of real doses

Using the average measured PM levels and kids activity pattern as inputs, the deposition of the three PM fractions was calculated for three regions of the respiratory tract (Head, Tracheobronchial (TB), and Pulmonary (P)) by the use of a dosimetry model (MPPD v 2.11 (ARA, 2014)). To calculate the real dose to use in the experiments, the total amount of PM reaching the pulmonary region was divided by 32 m^2 to obtain the mass of PM per alveolar area for an 8 years old kid (Dunnill, 1962). Then, this number was multiplied by the total surface of the chamber slide used for growing the cells (4.2 cm^2). All other parameters needed for the simulation were remained as described previously (Sánchez-Soberón et al., 2015).

2.5. Cell line and cytotoxicity assay

Lung carcinoma cells A549 (ATCC® CCL-185™) have been extensively used in toxicity of lung cells (L. Cao et al., 2015; Xu et al., 2013). To study the cytotoxicity of $PM_{2.5-0.25}$ and $PM_{0.25}$, an MTT assay was performed for each PM fraction separately (Roig et al., 2013). Cells were grown in Dulbecco's Modified Eagle's Medium, supplemented with 10 % inactivated Fetal Bovine Serum and 1 % penicillin in an incubator at 37 °C, 5 % CO_2 and saturating humidity. Following manufacturer recommendations, cells were seeded at a concentration of 4×10^3 cells/cm^2 in 96-well plates. After 48 h, cells were observed under phase contrast microscopy (Olympus, Japan) to ensure a confluence between 70 to 80%. Subsequently, medium was absorbed and replenished with fresh medium containing different concentrations of the PM extracts (500, 100, 50, 10, 5, 1, 0.5 and 0.1 µg/mL). Four replicates were used for every concentration, including negative controls. After PM

application, cells were left in contact with the medium containing the particles during 72 h.

After exposure, the MTT reagent was added to the wells to a final concentration of 5 %. The wells were incubated for 4 h until purple precipitate was visible. Subsequently, detergent was added to a final concentration of 50 % (*v/v)* and samples were left in the dark for 2 h. Absorbance was then measured at 570 nm using an Epoch 2 microplate spectrophotometer (BioTek, USA). To ensure reproducibility of the procedure, this experiment was done twice. LC_5 doses were calculated by using a biphasic equation from the dose-response scatter plot using the software Dr. Fit (Di Veroli et al., 2015).

2.6. Exposure strategy and metabolite extraction

Cells were seeded and grown in 4.2 cm^2 chamber slides under the same conditions described for the cytotoxicity assay (i.e. 37 °C, 5 % CO_2, saturating humidity, and plating density of 4×10^3 cells/cm^2). After 48 h of cell proliferation, medium was extracted, and cells were exposed to media containing, depending on the experiment, LC_5 or real dose of $PM_{2.5\text{-}0.25}$ and $PM_{0.25}$. Chamber slides were randomized for three exposure conditions: $PM_{2.5\text{-}0.25}$, $PM_{0.25}$ and control. Six replicates were done for every condition. Three independent experiments were conducted: one experiment, where the real dose was applied and two experiments where the LC_5 was used. (Further information regarding concentrations applied in each experiment can be seen in Table S1).

To extract the metabolites, we followed procedures previously published (Cuykx et al., 2017a, 2017b). In brief, after 72 h exposure, cells were washed twice with Phosphate Buffered Saline (PBS) and cell metabolism was quenched by submerging cells into liquid nitrogen. Chamber slides were then scraped three times with 200 µL of 80 % (v/v) MeOH/MilliQ-water and the content was transferred to a vial containing 420 µL of chloroform and 500 µL of milliQ-water, having a final solvent ratio of 2/3/2 water/MeOH/$CHCl_3$. The vials were then spiked with internal standards: 200 ng cholesterol-d4, and 100 ng 2-ethylhexyl phosphate (TEHP) and lauric acid-d3 for non-polar fraction, and 200 ng tryptophane-d5 and succinic acid-d4 for the polar fraction. Vials were then

vortexed three times for 30 s, and equilibrated for 10 min at 4 °C. Subsequently they were centrifuged at 3500 rpm during 7 min. The polar supernatant was transferred to pre-cooled Eppendorf tubes, while the lower, non-polar phase was transferred to vials containing chloroform. 40 µL of polar phase from each sample were put in two Eppendorfs to make a couple of quality control (QC) pools for polar compounds. Similarly, 20 µL of non-polar phase from each sample were aggregated into two vials to obtain two QC non-polar pools. Samples and QC were evaporated with nitrogen (non-polar phase) or using a centrifugal evaporator for 2.5 h (polar phase). Both, polar and non-polar samples were stored at -80 ºC prior to analysis.

2.7. Metabolomics Set-up:

Detail of the methods here employed can be consulted in Supplementary Materials. In brief, non-polar vials and polar Eppendorfs were divided into two subsamples: one was positively ionized and the other one was negatively ionized. This ionization methodology has proven to be successful for metabolomic studies, given the heterogeneity and complexity of biological samples (Nordström et al., 2008) Positive and negative non-polar vials were analyzed on a Kinetex XB-C18 (150 × 2.1 mm; 1.7 µm particle size, Phenomenex, Utrecht, the Netherlands). A mixture of MeOH, IPA, and NH_4Ac (pH 6.7) was used as mobile phase in negative ionization mode, while a mixture of ACN, IPA, and water with an acetate buffer (pH 4.2) was used as mobile phase in positive ionization mode. Positive polar Eppendorfs were analyzed using an iHILIC column (100 × 2.1 mm; 1.8 µm particle size, HILICON, Umea, Sweden) using ACN/MeOH and water with a NH_4F/FA buffer (pH 3.15) as mobile phase. Negative polar Eppendorfs were analyzed through a Gemini® Phenyl-hexyl column (150 × 2 mm, 3 µm particle size) (Phenomenex®, Torrence, CA, USA). Mobile phase was a mixture of MeOH, TBA and FA in MeOH/MilliQ water (pH=9). The columns were attached on an Agilent Infinity 1290 UPLC (Agilent Technologies, Santa Clara, USA), and the detection was performed in an Agilent 6530 QTOF with an Agilent Jet Stream nebulizer (Agilent Technologies).

2.8. Data treatment:

Mass-Hunter qualitative software (version 2.06.00, Agilent technologies) was used to evaluate LC and MS parameters. To extract internal standards from the chromatogram, the "Find by Formula"-algorithm (FBF) was used. Deconvolution algorithm was set to retain peaks having a quality score higher than 80% and abundance greater than 3000. These signals were subsequently grouped into molecular features according to their m/z, retention time, and correspondence to isotopes or adducts. Extracted features represent thus the different m/z signals of a metabolite. Mass Profiler (v12.5, Agilent Technologies, Santa Clara, CA, USA) was used to merge data coming from consecutive runs. The sums of the areas of all ions of the molecular features were the dependent values of the variables.

Features present in at least 80 % of the samples were retained for statistical analysis. This analysis was performed using the software EZ info v 2.0 (Umetrics, Umeå, Sweden). Principal Component Analysis (PCA) and Orthogonal Partial Least Squares-Discriminant Analysis (OPLS-DA) techniques were applied to estimate the quality of the dataset and to detect molecular features of interest respectively. Welch T tests with Benjamini-Hochberg correction were used to evaluate the significance of differences of PM levels among environments, PM fractions (cytotoxicity), and between exposed and control groups (metabolomic assays). Those differences were considered significant when the corrected p was below 0.05.

Annotation of significant features was performed using Molecular Formula Generator algorithm from the Mass-Hunter software. Tentative formulas were calculated having into account a mass error of 10 ppm, isotope spacing of 5 ppm, and a maximal 5 % difference in abundance compared to the calculated isotopic pattern. To find structures for these features, a search was performed in LipidMaps, Metlin, and Human Metabolome Database (HMDB) (Fahy et al., 2007; Smith et al., 2005; Wishart et al., 2013). The levels of confidence in identification are reported according to Schymanski et al. (2014). Heat maps were designed using the online resource Metaboanalyst v 4.0 (Xia and Wishart, 2016).

3. Results and discussion

3.1. PM levels and time activity pattern:

Concentrations of the three PM fractions measured in the different microenvironments can be seen on Figure 1.

Sensitivity in our samples was 0.39 $\mu g/m^3$, which introduces an uncertainty between 10 and 20% in $PM_{2.5\text{-}0.25}$ at home and outdoors. Average outdoor values obtained in this study were within the range of the average annual values reported by the Catalonian Administration during the last five years in the same area (Generalitat de Catalunya, 2017). Although not statistically significant, ($p>0.05$), average outdoor concentrations were higher than those registered during the same days by the air quality monitor stations in the area (16.6 and 9.3 $\mu g/m^3$ for PM_{10} and $PM_{2.5}$ respectively) (Generalitat de Catalunya, 2016). Average PM concentrations were below the thresholds set by the European legislation (i.e. daily average of 50 $\mu g/m^3$ for PM_{10}, and annual average of 40 $\mu g/m^3$ and 25 $\mu g/m^3$ for PM_{10} and $PM_{2.5}$ respectively) (European Commission and EU Parliament, 2008). The highest concentrations for every PM fraction were observed in classrooms, while the levels at home were the lowest. These results could be highly related with the occupancy of these microenvironments. The higher the human activity, the greater the resuspension and contribution of organic PM (textile fibers and skin debris) indoors (Serfozo et al., 2014; Viana et al., 2014). The low occupancy at home, in combination with the lack of ventilation and absence of other indoor sources in the room (i.e. tobacco, gas stove), could be the cause of experiencing lower PM levels at home than outdoors. This same trend has been reported previously for dwellings having similar characteristics to the one used in this study (Romagnoli et al., 2016; Xiao et al., 2018).

Regarding time activity patterns, share of time spent by students in the different microenvironments and performing the different activities can be seen on Figure 2:

Kids spent most of their time (90 %) indoors, while the outdoor time was mostly used during heavy intensity activities. The most time-demanding activity was sleeping (9.5 hours per day), while same

share of time was spent sitting in school and at home (5 hours each activity). Light exercise at home was performed for 2 hours a day, while only half an hour of light exercise outdoors was reported. Heavy exercise was fully performed outdoors, spending a daily average of 2 hours for this activity. The activity pattern obtained in the present study were similar to those obtained by other researchers in western countries (Cohen Hubal et al., 2000; Matz et al., 2015).

3.2. Deposition pattern of particles and real dose calculation

Daily deposited mass of the three sampled PM fractions can be seen on Table 1. The PM fraction registering the highest overall deposition masses was $PM_{10-2.5}$. This fraction was mostly deposited in the head and tracheobronchial regions of the respiratory tract, while, as seen in previous studies, the amount of coarse particles reaching the lung was minor (Sánchez-Soberón et al., 2015). Despite the scarce amount of time spent outdoors performing high intensity activities (2 hours per day), this activity reached the highest share of PM deposition regardless PM fraction. Fine fractions ($PM_{2.5-0.25}$ and $PM_{0.25}$), however, followed a different deposition pattern within the respiratory tract. Between 30 and 40 % of the total deposited mass of these fractions was addressed in the lung. Deposited mass of $PM_{2.5-0.25}$ in lungs reaches it maximum during class time. In the case of $PM_{0.25}$, heavy exercise outdoors is the activity registering the highest deposition masses for every respiratory region. Regardless of PM fraction studied, head region registered the highest deposition masses.

These variances in deposition patterns of the three PM fractions are related to the different levels of PM experienced in every environment, but also by the deposition mechanisms considered in the MPPD model: inertial impaction, sedimentation (gravitational setting), and diffusion (Brown et al., 2013). Impaction and sedimentation are the dominant mechanisms in particles bigger than 1 µm (Salma et al., 2015). These mechanisms are highly dependent on the air speed on the respiratory tract (Hussain et al., 2011). Thus, high air speeds will favor the impaction, while low velocities will favor sedimentation. Furthermore, the larger the PM, the more likely is to experience one of these processes. Diffusion mechanism appears in particles smaller than 0.5 µm, which behave like gas molecules. Particles within this size follow a Brownian motion, and they deposit at random (Bakand

et al., 2012).

In the first part of the respiratory tract, the speed of inhaled air reaches the highest velocity within the respiratory tract. Furthermore, as soon as the activity intensity increases, so does the air velocity. Consequently, impaction phenomenon is the dominant deposition mechanism in head region, affecting especially those particles of bigger size during high intensity activities (Hussain et al., 2011). Air passing through the tracheobronchial region experiences a deceleration, causing the sedimentation of the heaviest particles. When reaching terminal areas of the respiratory tract, the speed of air is minimal, which favors sedimentation. However, at this point, most of the coarse PM has been already deposited, and diffusion mechanism of $PM_{0.25}$ becomes the most important deposition process (CCOHS, 2010).

Based on these results, the amount of $PM_{2.5\text{-}0.25}$ and $PM_{0.25}$ deposited into the pulmonary region after 72 h would be 30.75 and 80.11 µg, respectively. To perform *in vitro* toxicity studies, the doses were converted to 0.27 ng/mL and 0.70 ng/mL of $PM_{2.5\text{-}0.25}$ and $PM_{0.25}$, respectively (Table S1).

3.3. Cytotoxicity

Since the mass of $PM_{10\text{-}2.5}$ reaching the lungs was negligible, toxicity assays were performed for $PM_{2.5\text{-}0.25}$ and $PM_{0.25}$. As reported in previous studies using same cell line and PM fractions, internalization of PM was reported in our cells (Figure S2)(Dominici et al., 2013). Dose-response plot graphs, as well as fitting equations for both PM fractions can be seen in Figure 3. Biphasic decay was the best fitting equation for our data, so it was chosen to calculate the concentration corresponding to 5% of mortality (LC_5). The smaller PM fraction causes a higher toxicity, especially when applying doses ranging from 0.5 to 10 µg/mL. Consequently, estimated LC_5 for $PM_{0.25}$ was lower than for $PM_{2.5\text{-}0.25}$ (8.08 ng/mL and 73.70 ng/mL respectively). It should be noted that in our case, these LC_5 values are out of the ranges of concentrations assessed in our cytotoxicity assay. Subsequent microscopic observations of cells after the use of these doses were performed, corroborating a slightly higher cell mortality than control cells, which is appropriate to perform

metabolomic assays. However, these values are an approach to real LC_5, and should not be taken as absolute values for this indicator. This trend of a higher toxicity of smaller PM has been reported before (L. Cao et al., 2015; Guan et al., 2016; Zou et al., 2017). In fact, this reduction in the size is related with a greater surface area, which can, apart from chemical composition, induce higher damage to cells (Kelly and Fussell, 2012).

Comparing our result with previous research is complicated. Few studies have been developed to evaluate the cytotoxicity of A549 cells after 72 h exposure to PM, and to our best knowledge, none of them has divided $PM_{2.5}$ into two fractions. Ho et al. (2016) obtained similar toxicity values (i.e. LC_{50}) after exposing A549 cells to $PM_{2.5}$ from coal burning origin. However, other studies using environmental or household $PM_{2.5}$ reported higher LC_{50} values (M. Huang et al., 2015; Q. Huang et al., 2015). Apart from differences in the PM fractions here assessed, differences between studies could be the result of different PM chemical composition and shape (data of these parameters for the present study is in preparation). Other factor influencing differences among studies is the diverse methodologies used in the above cited studies. Particulate matter collection media varies from fiber filters to PTFE membranes, and extraction of PM has been performed under ultrapure water or methanol. In the present study we decided to use PC filters for both, their ease in PM extraction without excessive mechanical means, and their hydrophilicity (Greenwell et al., 2002). This make them suitable to obtain PM aqueous solutions, as expected to find inside the lungs (Cross et al., 1994).

3.4. Metabolomics:

Regardless of experiment performed, between 1400 and 1600 non-polar features, and between 1100 and 1400 polar features per replicate were detected in the present study. These numbers are in line with the performance reported previously using the same methodology (Cuykx et al., 2017b).

3.4.1. *LC_5 experiment:*

After analyzing metabolic changes in exposed cells, those replicates treated with $PM_{0.25}$ LC_5

315 presented significant differences in the content of 39 metabolites compared to control cells (Tables
316 S2 and S3). On the other hand, cells exposed to $PM_{2.5\text{-}0.25}$ LC_5 showed significant differences in the
317 content of 38 features with respect to control replicates (Tables S4, and S5).

318 Hierarchical clustering analysis of these features, as well as the samples, can be seen in Figure 4.
319 According to this heat map, there is a grouping of samples into two marked groups: exposed and
320 control. At the same time, there are a couple of clusters within the exposed group: one exclusively
321 formed by 5 $PM_{0.25}$ replicates (green color dashed square), and the other comprising $PM_{2.5\text{-}0.25}$ and
322 the remaining $PM_{0.25}$ replicate (blue color dashed line). This last $PM_{0.25}$ replicate showed a
323 metabolic profile (i.e. fold change values in the altered metabolites) closer to the overall metabolic
324 profile displayed by cell exposed to $PM_{2.5\text{-}0.25}$. Regarding compounds, a disposition into two groups
325 was noted depending on the overall regulation pattern. The first group (yellow dot-dashed square)
326 contains mostly downregulated features in exposed cells, which comprised cardiolipins (CLs),
327 phosphatidylserines (PSs), and most of phosphatidylcholines (PCs). The second group (purple dot-
328 dashed square) is mainly formed by the upregulated features and includes all identified ceramides
329 (CERs).

330 Regardless of PM fraction applied, most of the altered metabolites were non-polar (Tables S2 and
331 S3). The vast majority of them were triglycerides (TG), CERs, and phospholipids. More
332 specifically, these changes have been detected for PSs, PCs, PEs, and CLs. These metabolites are
333 important constituents of cells membranes (Stillwell, 2016). Triglycerides and PCs are also the main
334 components of lung surfactant, a protein-lipid mixture essential to reduce tension at the alveoli air-
335 liquid interphase (Bernhard et al., 2001; Lopez-Rodriguez and Pérez-Gil, 2014).

336 Under normal conditions, PSs are located in the inner part of the plasma membrane. But in cells
337 undergoing the apoptosis process, these lipids turn to the external surface of the cell membrane,
338 sending a distress signal to macrophages in order to be phagocyted (Segawa and Nagata, 2015).
339 Consequently, these substances have been studied as biomarkers of different diseases, such as
340 cancer (Sharma and Kanwar, 2017). Although we were not able to locate where in the cell

membrane PSs were, we noticed a downregulation of this group of compounds in both ($PM_{2.5-0.25}$ and $PM_{0.25}$) exposed groups.

Phosphatidylethanolamines (PEs) play a significant role in membrane fusion and division, apoptosis, and autophagy (Pavlovic and Bakovic, 2013). Our results show significant downregulation in the content of most PEs regardless of PM fraction applied. Phosphatidylcholines (PCs), are the main component of lung surfactant (Bernhard et al., 2001). Cells exposed to $PM_{0.25}$ showed an overall upregulation in PC content, while those cells exposed to $PM_{2.5-0.25}$ showed an overall downregulation. This size related response in PC regulation has been previously reported in other studies (Chen et al., 2014; Juvin et al., 2002; Wang et al., 2017).

PCs and PEs are mainly generated via a couple of mechanisms (Figure 5): *de novo* or from PS decarboxylation (Bleijerveld et al., 2007; Vance, 2008). In *de-novo* pathway, PEs and PCs are generated from ethanolamine and choline, respectively. (Gibellini and Smith, 2010). The other pathway consists on the transformation of PS to PE via decarboxylation. This PE can be then transformed into PC by the action of phosphatidyl-ethanolamine N-methyltransferase (PEMT) (Zinrajh et al., 2014).

$PM_{2.5-0.25}$ elicits an overall downregulation on PSs, PEs, and PCs (Figure 5a). In mammalian cells, PSs are synthetized exclusively from PEs and PCs (Vance and Tasseva, 2013). Therefore, a decrease in the synthesis of PEs and PCs will lead to a decrease on PCs. Thus, $PM_{2.5-0.25}$ could be affecting the *de novo* pathway. On the other hand, $PM_{0.25}$ are more likely to affect the PS decarboxylation pathway, increasing the levels of PCs by transforming PSs to PEs, and PEs into PCs (Figure 5b). These differences in the way of action between $PM_{2.5-0.25}$ and $PM_{0.25}$ could be due to differences in physicochemical characteristics between these two fractions.

A downregulation in CLs was significant in this study, regardless of the PM fraction exposed. CLs are almost exclusively localized in the inner mitochondrial membrane (Houtkooper and Vaz, 2008). Cardiolipins improve the ATP generation via oxidative phosphorylation within this organelle, apart

from being involved in other mitochondrial processes (Claypool and Koehler, 2012). , and more specifically, its polar toxic constituents have been recognized previously as disruptors of mitochondrial functions (Xia et al., 2004). Although using different kind of cells, Hiura et al. (2000) also recorded a decrease in mitochondrial CLs after exposing mice macrophages to PM. This damage in the mitochondrial membrane could be generated by the particle surface (mechanical damage), or by formation of reactive oxygen species (ROS) (von Moos and Slaveykova, 2014).

Ceramides are highly concentrated in cell membranes and play a significant role in the response to stress stimuli (Bikman and Summers, 2011). The upregulation of CERs is recognized as a signal of apoptosis and has been related to several lung diseases (Lee et al., 2015; Petrache et al., 2005). Previous studies reported clear upregulations of CERs after PM exposures (Peuschel et al., 2012; Zhang et al., 2017). However, the regulations of these CERs were variable, and fold changes were low. This difference could be explained by the PM doses applied in the present study, which were lower than the previously reported papers.

Regarding polar constituents (Tables S4 and S5), cells exposed to $PM_{2.5-0.25}$ showed an upregulation in N1-Acetylspermidine, a precursor of spermidine (Wishart et al., 2013). Spermidine is involved in regulation of inflammatory reactions, and has been recognized as defense line against reactive oxygen species and DNA protector in lungs (Hoet and Nemery, 2000). On the other hand, cells exposed to $PM_{0.25}$ showed and upregulation in 1-Pyrroline-5-carboxylic acid. This compound is a precursor, of L-proline, which is able to generate specific reactive oxygen species (ROS) acting as signals for tumor suppression, apoptosis and cell survival (Liang et al., 2013; Wishart et al., 2013). Furthermore, proline metabolism can be used as a source of energy under stress conditions within cells (Phang et al., 2015).

3.4.2. *Real dose experiment*

When cells were exposed to realistic PM doses, the number of significant features had been reduced to 10 for $PM_{0.25}$ and 5 for $PM_{2.5-0.25}$ (Tables S5 and S6). Under real conditions, $PM_{0.25}$ doses are

391 higher than $PM_{2.5-0.25}$, and consequently a higher effect of these particles to the cells could be
392 observed.

393 As shown in Figure 6, hierarchical grouping of replicates is not as clear as during the LC_5 exposure.
394 Replicates are distributed into two groups: the first comprising exposed cells of both PM fractions,
395 while the second comprises a mix of exposed and control cells. Nevertheless, a plausible tendency
396 in sample distribution can be drawn: exposure to PM tend to cluster in comparison to control
397 samples. There is also a grouping in compounds: in a first group it is possible to differentiate those
398 features upregulated in the exposed cells (yellow dot-dashed square), while the second group
399 comprises those compounds showing fold changes dependent on the used PM (purple dot-dashed
400 square).

401 Contrary to the LC_5 experiment, the number of affected features after $PM_{0.25}$ exposure was higher
402 for polar (7) than for non-polar (3), which could reveal less intensive effects on cell membranes.
403 Cells exposed to $PM_{0.25}$ experienced an upregulation in the content of most altered metabolites,
404 such as proline, TGs, and PEs. These results could indicate that cells are undergoing a hormesis
405 phase, in which cells are activated as a consequence of being exposed to low doses of toxic agents
406 (Zimmermann et al., 2014). Cells exposed to $PM_{2.5-0.25}$ showed an overall decrease in the altered
407 metabolites. Slight downregulations were noticed for PEs and phosphatidylglycerols (PGs), one of
408 the constituents of lung surfactant and also present at small scale in cell membranes (Stillwell,
409 2016). However, as previously pointed out, the number of altered metabolites in this experiment
410 was small, showing a higher fold change variability among the same exposure group replicates.

411 Despite the promising results of the approach here described, this study still presents some
412 limitations that should be faced in future studies. First, the number of students surveyed, the number
413 of environments assessed, and sampling duration should be increased to obtain wider conclusions.
414 Uncertainty in $PM_{2.5-0.25}$ levels should be decreased by either, increasing sampling time or using a
415 more sensitive balance. Regarding *in-vitro* assays, a more accurate calculation of LC_5 is needed, as
416 pointed out previously. Also, having access to a PM-controlled air chamber would be useful to

obtain more appropriate negative controls. Finally, to simplify dosage strategy, real doses were calculated having into account the total surface of the culture dishes, instead of the percentage of cell confluence.

4. Conclusions

Three fractions of PM ($PM_{0.25}$, $PM_{2.5-0.25}$, and $PM_{10-2.5}$) were collected in three environments (outdoor, classroom, and home) within a village located nearby an industrial complex. The time activity patterns of 20 students attending school were obtained to study the exposure and deposition of PM within the children's respiratory tract. Afterwards, these particles were extracted from filters and put in contact with alveolar A549 cells to study the cytotoxicity and changes in the metabolic profile after 72 h exposure. Classroom microenvironment registered the highest levels of every PM fraction collected, due to its higher occupancy. Regardless of PM fraction, the upper respiratory tract (head) was the region that retained most of the overall deposited mass, especially when performing heavy intensity activities. The finest fraction ($PM_{0.25}$) elicited a higher cytotoxicity than $PM_{2.5-0.25}$. The number of metabolites affected by particles exposure was similar for both fractions in LC_5 doses, while after applying real doses changes were mainly due to $PM_{0.25}$. These changes were mostly in compounds dealing with cell and mitochondrial membrane functions, revealing the potential of PM to elicit both extracellular and intracellular damage.

Acknowledgments

This study was financed by the Spanish Ministry of Economy and Competitiveness (MINECO) as part of the project CTM2015-65303-P. Francisco Sánchez-Soberón received a doctoral scholarship and an internship grant from the same organism.

References

ARA, 2014. ARA :: Products :: MPPD [WWW Document]. URL http://www.ara.com/products/mppd.htm (accessed 8.24.15).

Bakand, S., Hayes, A., Dechsakulthorn, F., 2012. Nanoparticles: a review of particle toxicology

following inhalation exposure. Inhal. Toxicol. 24, 125–135.

Bernhard, W., Hoffmann, S., Dombrowsky, H., Rau, G.A., Kamlage, A., Kappler, M., Haitsma, J.J., Freihorst, J., von der Hardt, H., Poets, C.F., 2001. Phosphatidylcholine Molecular Species in Lung Surfactant. Am. J. Respir. Cell Mol. Biol. 25, 725–731. doi:10.1165/ajrcmb.25.6.4616

Bikman, B.T., Summers, S.A., 2011. Ceramides as modulators of cellular and whole-body metabolism. J. Clin. Invest. doi:10.1172/JCI57144

Bleijerveld, O.B., Brouwers, J.F.H.M., Vaandrager, A.B., Helms, J.B., Houweling, M., 2007. The CDP-ethanolamine Pathway and Phosphatidylserine Decarboxylation Generate Different Phosphatidylethanolamine Molecular Species. J. Biol. Chem. 282, 28362–28372. doi:10.1074/jbc.M703786200

Brown, J.S., Gordon, T., Price, O., Asgharian, B., 2013. Thoracic and respirable particle definitions for human health risk assessment. Part. Fibre Toxicol. 10, 12. doi:10.1186/1743-8977-10-12

Cao, L., Zeng, J., Liu, K., Bao, L., Li, Y., 2015. Characterization and Cytotoxicity of PM<0.2, PM0.2–2.5 and PM2.5–10 around MSWI in Shanghai, China. Int. J. Environ. Res. Public Health 12, 5076–5089. doi:10.3390/ijerph120505076

Cao, X., Lin, H., Muskhelishvili, L., Latendresse, J., Richter, P., Heflich, R.H., 2015. Tight junction disruption by cadmium in an in vitro human airway tissue model. Respir. Res. 16, 30. doi:10.1186/s12931-015-0191-9

CCOHS, 2010. How Do Particulates Enter the Respiratory System? [WWW Document]. Can. Cent. Occup. Heal. Saf. URL https://www.ccohs.ca/oshanswers/chemicals/how_do.html (accessed 1.4.18).

Chen, M., Li, B., Sang, N., 2017. Particulate matter (PM2.5) exposure season-dependently induces neuronal apoptosis and synaptic injuries. J. Environ. Sci. (China) 54, 336–345. doi:10.1016/j.jes.2016.10.013

Chen, W.-L., Lin, C.-Y., Yan, Y.-H., Cheng, K.T., Cheng, T.-J., 2014. Alterations in rat pulmonary phosphatidylcholines after chronic exposure to ambient fine particulate matter. Mol. BioSyst.

10, 3163–3169. doi:10.1039/C4MB00435C

Claypool, S.M., Koehler, C.M., 2012. The complexity of cardiolipin in health and disease. Trends Biochem. Sci. 37, 32–41. doi:10.1016/j.tibs.2011.09.003

Cohen Hubal, E.A., Sheldon, L.S., Burke, J.M., McCurdy, T.R., Berry, M.R., Rigas, M.L., Zartarian, V.G., Freeman, N.C., 2000. Children's exposure assessment: a review of factors influencing Children's exposure, and the data available to characterize and assess that exposure. Environ. Health Perspect. 108, 475–486.

Cross, C.E., van der Vliet, A., O'Neill, C.A., Louie, S., Halliwell, B., 1994. Oxidants, antioxidants, and respiratory tract lining fluids. Environ. Health Perspect. 185–91.

Cuykx, M., Mortelé, O., Rodrigues, R.M., Vanhaecke, T., Covaci, A., 2017a. Optimisation of in vitro sample preparation for LC-MS metabolomics applications on HepaRG cell cultures. Anal. Methods 9, 3704–3712. doi:10.1039/C7AY00573C

Cuykx, M., Negreira, N., Beirnaert, C., Van den Eede, N., Rodrigues, R., Vanhaecke, T., Laukens, K., Covaci, A., 2017b. Tailored liquid chromatography–mass spectrometry analysis improves the coverage of the intracellular metabolome of HepaRG cells. J. Chromatogr. A 1487, 168–178. doi:10.1016/j.chroma.2017.01.050

Di Veroli, G.Y., Fornari, C., Goldlust, I., Mills, G., Koh, S.B., Bramhall, J.L., Richards, F.M., Jodrell, D.I., 2015. An automated fitting procedure and software for dose-response curves with multiphasic features. Sci. Rep. 5, 14701. doi:10.1038/srep14701

Dominici, L., Guerrera, E., Villarini, M., Fatigoni, C., Moretti, M., Blasi, P., Monarca, S., 2013. Evaluation of in vitro cytoxicity and genotoxicity of size-fractionated air particles sampled during road tunnel construction. Biomed Res. Int. 2013, 1–9. doi:10.1155/2013/345724

Donahue, N.M., Posner, L.N., Westervelt, D.M., Li, Z., Shrivastava, M., Presto, A.A., Sullivan, R.C., Adams, P.J., Pandis, S.N., Robinson, A.L., Donahue, N.M., Posner, L.N., Westervelt, D.M., Li, Z., Shrivastava, M., Presto, A.A., Sullivan, R.C., Adams, P.J., Pandis, S.N., Robinson, A.L., 2016. Where Did This Particle Come From? Sources of Particle Number and

494 Mass for Human Exposure Estimates, in: Hester, R.E., Harrison, R.M., Querol, X. (Eds.),
495 Airborne Particulate Matter: Sources, Atmospheric Processess and Health. pp. 35–71.
496 doi:10.1039/9781782626589-00035
497 Dunnill, M.S., 1962. Postnatal Growth of the Lung. Thorax 17, 329–333. doi:10.1136/thx.17.4.329
498 European Commission, EU Parliament, 2008. Directive 2008/50/EC of the European Parliament
499 and of the Council of 21 May 2008 on ambient air quality and cleaner air for Europe. Off. J.
500 Eur. Communities. 152, 1–44.
501 Fahy, E., Sud, M., Cotter, D., Subramaniam, S., 2007. LIPID MAPS online tools for lipid research.
502 Nucleic Acids Res. 35, W606-12. doi:10.1093/nar/gkm324
503 Generalitat de Catalunya, 2017. La qualitat de l'aire a Catalunya [WWW Document]. URL
504 http://www.qualitatdelaire.cat/contaminant/cerca/7/4/14.html (accessed 6.4.18).
505 Generalitat de Catalunya, 2016. Dades de qualitat de l'aire v 1.2.8 [WWW Document]. URL
506 http://dtes.gencat.cat/icqa/ (accessed 6.4.18).
507 Gibellini, F., Smith, T.K., 2010. The Kennedy pathway-De novo synthesis of
508 phosphatidylethanolamine and phosphatidylcholine. IUBMB Life 62, n/a-n/a.
509 doi:10.1002/iub.337
510 Greenwell, L.L., Jones, T.P., Richards, R.J., 2002. The collection of PM10for toxicological
511 investigation: Comparisons between different collecting devices. Environ. Monit. Assess. 79,
512 251–273. doi:10.1023/A:1020230727359
513 Guan, L., Rui, W., Bai, R., Zhang, W., Zhang, F., Ding, W., 2016. Effects of Size-Fractionated
514 Particulate Matter on Cellular Oxidant Radical Generation in Human Bronchial Epithelial
515 BEAS-2B Cells. Int. J. Environ. Res. Public Health 13, 483. doi:10.3390/ijerph13050483
516 Hiura, T.S., Li, N., Kaplan, R., Horwitz, M., Seagrave, J.-C., Nel, A.E., 2000. The Role of a
517 Mitochondrial Pathway in the Induction of Apoptosis by Chemicals Extracted from Diesel
518 Exhaust Particles. J. Immunol. 165, 2703–2711. doi:10.4049/jimmunol.165.5.2703
519 Ho, K.F., Chang, C.C., Tian, L., Chan, C.S., Musa Bandowe, B.A., Lui, K.H., Lee, K.Y., Chuang,

K.J., Liu, C.Y., Ning, Z., Chuang, H.C., 2016. Effects of polycyclic aromatic compounds in fine particulate matter generated from household coal combustion on response to EGFR mutations in vitro. Environ. Pollut. 218, 1262–1269. doi:10.1016/j.envpol.2016.08.084

Hoet, P.H., Nemery, B., 2000. Polyamines in the lung: polyamine uptake and polyamine-linked pathological or toxicological conditions. Am. J. Physiol. Lung Cell. Mol. Physiol. 278, L417-33.

Horgan, R.P., Kenny, L.C., 2011. "Omic" technologies: genomics, transcriptomics, proteomics and metabolomics. Obstet. Gynaecol. 13, 189–195. doi:10.1576/toag.13.3.189.27672

Houtkooper, R.H., Vaz, F.M., 2008. Cardiolipin, the heart of mitochondrial metabolism. Cell. Mol. Life Sci. 65, 2493–2506. doi:10.1007/s00018-008-8030-5

Huang, M., Kang, Y., Wang, W., Chan, C.Y., Wang, X., Wong, M.H., 2015. Potential cytotoxicity of water-soluble fraction of dust and particulate matters and relation to metal(loid)s based on three human cell lines. Chemosphere 135, 61–66. doi:10.1016/j.chemosphere.2015.04.004

Huang, Q., Zhang, J., Luo, L., Wang, X., Wang, X., Alamdar, A., Peng, S., Liu, L., Tian, M., Shen, H., 2015. Metabolomics reveals disturbed metabolic pathways in human lung epithelial cells exposed to airborne fine particulate matter. Toxicol. Res. 4, 939–947. doi:10.1039/C5TX00003C

Hussain, M., Madl, P., Khan, A., 2011. Lung deposition predictions of airborne particles and the emergence of contemporary diseases, Part-I. Health (Irvine. Calif). 2, 51–59.

Juvin, P., Fournier, T., Grandsaigne, M., Desmonts, J.-M., Aubier, M., 2002. Diesel particles increase phosphatidylcholine release through a NO pathway in alveolar type II cells. Am. J. Physiol. - Lung Cell. Mol. Physiol. 282, L1075–L1081. doi:10.1152/ajplung.00213.2001

Kelly, F., Fussell, J., 2016. Health Effects of Airborne Particles in Relation to Composition, Size and Source, in: Airborne Particulate Matter: Sources, Atmospheric Processess and Health. pp. 344–372.

Kelly, F.J., Fussell, J.C., 2012. Size, source and chemical composition as determinants of toxicity

attributable to ambient particulate matter. Atmos. Environ. 60, 504–526. doi:10.1016/j.atmosenv.2012.06.039

Lee, J., Yeganeh, B., Ermini, L., Post, M., 2015. Sphingolipids as cell fate regulators in lung development and disease. Apoptosis 20, 740–757. doi:10.1007/s10495-015-1112-6

Liang, X., Zhang, L., Natarajan, S.K., Becker, D.F., 2013. Proline mechanisms of stress survival. Antioxid. Redox Signal. 19, 998–1011. doi:10.1089/ars.2012.5074

Líbalová, H., Uhlířová, K., Kléma, J., Machala, M., Šrám, R.J., Ciganek, M., Topinka, J., 2012. Global gene expression changes in human embryonic lung fibroblasts induced by organic extracts from respirable air particles. Part. Fibre Toxicol. 9, 1. doi:10.1186/1743-8977-9-1

Longhin, E., Capasso, L., Battaglia, C., Proverbio, M.C., Cosentino, C., Cifola, I., Mangano, E., Camatini, M., Gualtieri, M., 2016. Integrative transcriptomic and protein analysis of human bronchial BEAS-2B exposed to seasonal urban particulate matter. Environ. Pollut. 209, 87–98. doi:10.1016/j.envpol.2015.11.013

Lopez-Rodriguez, E., Pérez-Gil, J., 2014. Structure-function relationships in pulmonary surfactant membranes: From biophysics to therapy. Biochim. Biophys. Acta - Biomembr. 1838, 1568–1585. doi:10.1016/j.bbamem.2014.01.028

MAPAMA, 2018. Inventario de instalaciones - Inventario Completo [WWW Document]. URL http://www.prtr-es.es/Informes/InventarioInstalacionesIPPC.aspx (accessed 2.19.18).

Matz, C.J., Stieb, D.M., Brion, O., 2015. Urban-rural differences in daily time-activity patterns, occupational activity and housing characteristics. Environ. Heal. 14, 88. doi:10.1186/s12940-015-0075-y

Megido, L., Suárez-Peña, B., Negral, L., Castrillón, L., Suárez, S., Fernández-Nava, Y., Marañón, E., 2016. Relationship between physico-chemical characteristics and potential toxicity of PM10. Chemosphere 162, 73–79. doi:10.1016/j.chemosphere.2016.07.067

Mesquita, S.R., Van Drooge, B.L., Oliveira, E., Grimalt, J.O., Barata, C., Vieira, N., Guimarães, L., Piña, B., 2015. Differential embryotoxicity of the organic pollutants in rural and urban air

572 particles. Environ. Pollut. 206, 535–542. doi:10.1016/j.envpol.2015.08.008
573 Nordström, A., Want, E., Northen, T., Lehtiö, J., Siuzdak, G., 2008. Multiple Ionization Mass
574 Spectrometry Strategy Used To Reveal the Complexity of Metabolomics. Anal. Chem. 80,
575 421–429. doi:10.1021/ac701982e
576 Pavlovic, Z., Bakovic, M., 2013. Regulation of Phosphatidylethanolamine Homeostasis—The
577 Critical Role of CTP:Phosphoethanolamine Cytidylyltransferase (Pcyt2). Int. J. Mol. Sci. 14,
578 2529–50. doi:10.3390/ijms14022529
579 Peixoto, M.S., de Oliveira Galvão, M.F., Batistuzzo de Medeiros, S.R., 2017. Cell death pathways
580 of particulate matter toxicity. Chemosphere. doi:10.1016/j.chemosphere.2017.08.076
581 Petrache, I., Natarajan, V., Zhen, L., Medler, T.R., Richter, A.T., Cho, C., Hubbard, W.C.,
582 Berdyshev, E. V, Tuder, R.M., 2005. Ceramide upregulation causes pulmonary cell apoptosis
583 and emphysema-like disease in mice. Nat. Med. 11, 491–498. doi:10.1038/nm1238
584 Peuschel, H., Sydlik, U., Grether-Beck, S., Felsner, I., Stöckmann, D., Jakob, S., Kroker, M.,
585 Haendeler, J., Gotić, M., Bieschke, C., Krutmann, J., Unfried, K., 2012. Carbon nanoparticles
586 induce ceramide- and lipid raft-dependent signalling in lung epithelial cells: A target for a
587 preventive strategy against environmentally-induced lung inflammation. Part. Fibre Toxicol. 9,
588 48. doi:10.1186/1743-8977-9-48
589 Phang, J.M., Liu, W., Hancock, C.N., Fischer, J.W., 2015. Proline metabolism and cancer. Curr.
590 Opin. Clin. Nutr. Metab. Care 18, 71–77. doi:10.1097/MCO.0000000000000121
591 Roig, N., Sierra, J., Rovira, J., Schuhmacher, M., Domingo, J.L., Nadal, M., 2013. In vitro tests to
592 assess toxic effects of airborne PM(10) samples. Correlation with metals and chlorinated
593 dioxins and furans. Sci. Total Environ. 443, 791–797. doi:10.1016/j.scitotenv.2012.11.022
594 Romagnoli, P., Balducci, C., Perilli, M., Vichi, F., Imperiali, A., Cecinato, A., 2016. Indoor air
595 quality at life and work environments in Rome, Italy. Environ. Sci. Pollut. Res. 23, 3503–3516.
596 doi:10.1007/s11356-015-5558-4
597 Salma, I., Füri, P., Németh, Z., Balásházy, I., Hofmann, W., Farkas, Á., 2015. Lung burden and

598 deposition distribution of inhaled atmospheric urban ultrafine particles as the first step in their
599 health risk assessment. Atmos. Environ. 104, 39–49. doi:10.1016/j.atmosenv.2014.12.060
600 Sánchez-Soberón, F., Mari, M., Kumar, V., Rovira, J., Nadal, M., Schuhmacher, M., 2015. An
601 approach to assess the Particulate Matter exposure for the population living around a cement
602 plant: modelling indoor air and particle deposition in the respiratory tract. Environ. Res. 143,
603 10–18. doi:10.1016/j.envres.2015.09.008
604 Schymanski, E.L., Jeon, J., Gulde, R., Fenner, K., Ruff, M., Singer, H.P., Hollender, J., 2014.
605 Identifying small molecules via high resolution mass spectrometry: Communicating
606 confidence. Environ. Sci. Technol. doi:10.1021/es5002105
607 Segawa, K., Nagata, S., 2015. An Apoptotic “Eat Me” Signal: Phosphatidylserine Exposure. Trends
608 Cell Biol. 25, 639–650. doi:10.1016/j.tcb.2015.08.003
609 Serfozo, N., Chatoutsidou, S.E., Lazaridis, M., 2014. The effect of particle resuspension during
610 walking activity to PM10 mass and number concentrations in an indoor microenvironment.
611 Build. Environ. 82, 180–189. doi:http://dx.doi.org/10.1016/j.buildenv.2014.08.017
612 Sharma, B., Kanwar, S.S., 2017. Phosphatidylserine: A cancer cell targeting biomarker. Semin.
613 Cancer Biol. doi:10.1016/j.semcancer.2017.08.012
614 Smith, C.A., O’Maille, G., Want, E.J., Qin, C., Trauger, S.A., Brandon, T.R., Custodio, D.E.,
615 Abagyan, R., Siuzdak, G., 2005. METLIN: a metabolite mass spectral database. Ther. Drug
616 Monit. 27, 747–51.
617 Stillwell, W., 2016. Membrane Polar Lipids, in: An Introduction to Biological Membranes. Elsevier,
618 pp. 63–87. doi:10.1016/B978-0-444-63772-7.00005-1
619 US EPA, 2016. Basic Information | Particulate Matter | Air & Radiation | US EPA [WWW
620 Document]. URL https://www.epa.gov/pm-pollution/particulate-matter-pm-basics#PM
621 (accessed 5.31.15).
622 Vaccari, M., Mascolo, M.G., Rotondo, F., Morandi, E., Quercioli, D., Perdichizzi, S., Zanzi, C.,
623 Serra, S., Poluzzi, V., Angelini, P., Grilli, S., Colacci, A., 2015. Identification of pathway-based

toxicity in the BALB/c 3T3 cell model. Toxicol. Vitr. 29, 1240–1253. doi:10.1016/j.tiv.2014.10.002

van Drooge, B.L., Marqueño, A., Grimalt, J.O., Fernández, P., Porte, C., 2017. Comparative toxicity and endocrine disruption potential of urban and rural atmospheric organic PM1in JEG-3 human placental cells. Environ. Pollut. 230, 378–386. doi:10.1016/j.envpol.2017.06.025

Vance, J.E., 2008. Thematic Review Series: Glycerolipids. Phosphatidylserine and phosphatidylethanolamine in mammalian cells: two metabolically related aminophospholipids. J. Lipid Res. 49, 1377–1387. doi:10.1194/jlr.R700020-JLR200

Vance, J.E., Tasseva, G., 2013. Formation and function of phosphatidylserine and phosphatidylethanolamine in mammalian cells. Biochim. Biophys. Acta - Mol. Cell Biol. Lipids. doi:10.1016/j.bbalip.2012.08.016

Viana, M., Rivas, I., Querol, X., Alastuey, A., Álvarez-Pedrerol, M., Bouso, L., Sioutas, C., Sunyer, J., 2014. Partitioning of trace elements and metals between quasi-ultrafine, accumulation and coarse aerosols in indoor and outdoor air in schools. Atmos. Environ. 106, 392–401. doi:10.1016/j.atmosenv.2014.07.027

von Moos, N., Slaveykova, V.I., 2014. Oxidative stress induced by inorganic nanoparticles in bacteria and aquatic microalgae – state of the art and knowledge gaps. Nanotoxicology 8, 605–630. doi:10.3109/17435390.2013.809810

Wang, X., Jiang, S., Liu, Y., Du, X., Zhang, W., Zhang, J., Shen, H., 2017. Comprehensive pulmonary metabolome responses to intratracheal instillation of airborne fine particulate matter in rats. Sci. Total Environ. 592, 41–50. doi:10.1016/j.scitotenv.2017.03.064

Wheelock, C.E., Goss, V.M., Balgoma, D., Nicholas, B., Brandsma, J., Skipp, P.J., Snowden, S., Burg, D., D'Amico, A., Horvath, I., Chaiboonchoe, A., Ahmed, H., Ballereau, S., Rossios, C., Chung, K.F., Montuschi, P., Fowler, S.J., Adcock, I.M., Postle, A.D., Dahlén, S.-E., Rowe, A., Sterk, P.J., Auffray, C., Djukanovic, R., 2013. Application of 'omics technologies to biomarker discovery in inflammatory lung diseases. Eur. Respir. J. 42, 802–825.

650 doi:10.1183/09031936.00078812

651 WHO, 2014. WHO | Ambient (outdoor) air quality and health [WWW Document]. WHO. URL

652 http://www.who.int/mediacentre/factsheets/fs313/en/ (accessed 6.21.16).

653 Wishart, D.S., Jewison, T., Guo, A.C., Wilson, M., Knox, C., Liu, Y., Djoumbou, Y., Mandal, R.,

654 Aziat, F., Dong, E., Bouatra, S., Sinelnikov, I., Arndt, D., Xia, J., Liu, P., Yallou, F., Bjorndahl,

655 T., Perez-Pineiro, R., Eisner, R., Allen, F., Neveu, V., Greiner, R., Scalbert, A., 2013. HMDB

656 3.0--The Human Metabolome Database in 2013. Nucleic Acids Res. 41, D801–D807.

657 doi:10.1093/nar/gks1065

658 Wu, W., Jin, Y., Carlsten, C., 2018. Inflammatory health effects of indoor and outdoor particulate

659 matter. J. Allergy Clin. Immunol. 141, 845. doi:10.1016/j.jaci.2018.01.014

660 Xia, J., Wishart, D.S., 2016. Using metaboanalyst 3.0 for comprehensive metabolomics data

661 analysis. Curr. Protoc. Bioinforma. 2016, 14.10.1-14.10.91. doi:10.1002/cpbi.11

662 Xia, T., Korge, P., Weiss, J.N., Li, N., Venkatesen, M.I., Sioutas, C., Nel, A., 2004. Quinones and

663 Aromatic Chemical Compounds in Particulate Matter Induce Mitochondrial Dysfunction:

664 Implications for Ultrafine Particle Toxicity. Environ. Health Perspect. 112, 1347–1358.

665 doi:10.1289/ehp.7167

666 Xiao, Y., Wang, L., Yu, M., Shui, T., Liu, L., Liu, J., 2018. Characteristics of indoor/outdoor

667 PM2.5and related carbonaceous species in a typical severely cold city in China during heating

668 season. Build. Environ. 129, 54–64. doi:10.1016/j.buildenv.2017.12.007

669 Xu, W., Jiang, J., Yang, B., Mei, D., Dai, B., 2013. ^{o}. Huanjing Kexue Xuebao/Acta Sci.

670 Circumstantiae 33, 3407–3412.

671 Zhang, S.-Y., Shao, D., Liu, H., Feng, J., Feng, B., Song, X., Zhao, Q., Chu, M., Jiang, C., Huang,

672 W., Wang, X., 2017. Metabolomics analysis reveals that benzo[a]pyrene, a component of PM

673 2.5 , promotes pulmonary injury by modifying lipid metabolism in a phospholipase A2-

674 dependent manner in vivo and in vitro. Redox Biol. 13, 459–469.

675 doi:10.1016/j.redox.2017.07.001

Zimmermann, A., Bauer, M.A., Kroemer, G., Madeo, F., Carmona-Gutierrez, D., 2014. When less is more : hormesis against stress and disease. Microb. Cell 1, 150–153. doi:doi:

Zinrajh, D., Hörl, G., Jürgens, G., Marc, J., Sok, M., Cerne, D., 2014. Increased phosphatidylethanolamine N-methyltransferase gene expression in non-small-cell lung cancer tissue predicts shorter patient survival. Oncol. Lett. 7, 2175–2179. doi:10.3892/ol.2014.2035

Zou, Y., Wu, Y., Wang, Y., Li, Y., Jin, C., 2017. Physicochemical properties, in vitro cytotoxic and genotoxic effects of PM1.0 and PM2.5 from Shanghai, China. Environ. Sci. Pollut. Res. 24, 19508–19516. doi:10.1007/s11356-017-9626-9

Figure 1: Average levels of PM within the three microenvironments. Error bars denote standard deviations among samples (n=4). Asterisks denote statistically significant differences ($p<0.05$).

Figure 2: Average daily share of time of the students attending to the school (n=20).

Figure 3: Dose-response graph of A549 cells after 72 h exposure to $PM_{2.5-0.25}$ (red) and $PM_{0.25}$ (blue). The curve was fitted using a two-phase decay. Error bars denote standard deviations (n=4). Characters indicate statistically significant differences between the two fractions at a given dose (a = $p<0.05$; b= $p<0.01$).

Figure 4: Hierarchical clustering heatmap analysis of significative differential metabolites after LC_5 exposure. Metabolite fold changes with respect to control cells range between deep blue (negative fold changes) to deep red (positive fold changes). Red dashed square embeds the control cluster, blue dashed square embeds the cluster comprising all $PM_{2.5-0.25}$ and one $PM_{0.25}$ replicate, and green dashed line embeds the remaining $PM_{0.25}$replicates. Yellow dot-dashed square embeds those features mostly downregulated in exposed cells, while purple dot-dashed square embeds those features mostly upregulated in exposed cells.

Figure 5: Observed PS, PE, and PC changes after exposure to $PM_{2.5-0.25}$ (a) and $PM_{0.25}$ (b). Upregulated metabolites are shown in green background, while downregulated metabolites are shown in red. Key: Cho, choline; Etn, ethanolamine; PC, phosphatidylcholine; PE, phosphatidylethanolamine; PEMT, phosphatidyl-ethanolamine N-methyltransferase; PS, phosphatidylserine; Ser, serine.

Figure 6: Hierarchical clustering heatmap analysis of significative differential metabolites after real dose exposure. Metabolite fold changes with respect to control cells range between deep blue (negative fold changes) to deep red (positive fold

changes). Blue dashed square embeds most of the exposed replicates, while red dashed square embeds control cells plus remaining exposed replicates. Yellow dot-dashed square embeds those features mostly downregulated in exposed cells, while purple dot-dashed square embeds those features mostly upregulated in exposed cells.

Table 1: Daily deposited doses calculated for every PM fraction and respiratory region (µg/day).

		$PM_{10-2.5}$				$PM_{2.5-0.25}$				$PM_{0.25}$				Total
Activity	**Environment**	**Head**	**TB[1]**	**P[2]**	**Total**	**Head**	**TB**	**P**	**Total**	**Head**	**TB**	**P**	**Total**	
Sleeping	Home	11.24	5.44	0.3	16.98	1.6	0.34	2.4	4.34	4.98	1.3	5.7	11.98	33.31
Sitting	Classroom	18.88	8.51	0.17	27.56	3.21	0.71	4.45	8.37	5.86	1.46	6.35	13.67	49.6
Sitting	Home	7.55	3.41	0.07	11.03	1.07	0.24	1.48	2.79	3.3	0.82	3.57	7.69	21.5
Light intensity	Home	10.67	2.63	0	13.3	1.5	1	0.91	3.41	4.51	1.01	3.34	8.86	25.57
Light intensity	Outdoors	3.11	0.77	0	3.88	0.56	0.38	0.34	1.28	1.5	0.34	1.11	2.95	8.11
Heavy intensity	Outdoors	24.28	4.01	0	28.29	3.97	6.09	0.66	10.72	11.89	2.68	6.63	21.2	60.2
Total		75.72	24.77	0.54	101.03	11.91	8.75	10.25	30.91	32.05	7.6	26.7	66.35	198.29

[1] TB: Tracheobronchial; [2] P: Pulmonary (Lung).

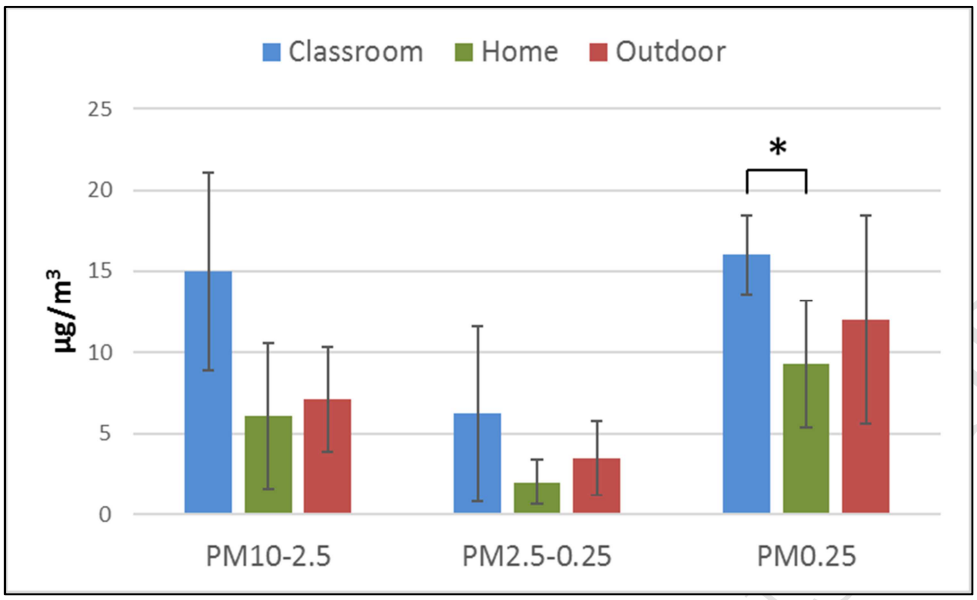

Figure 1

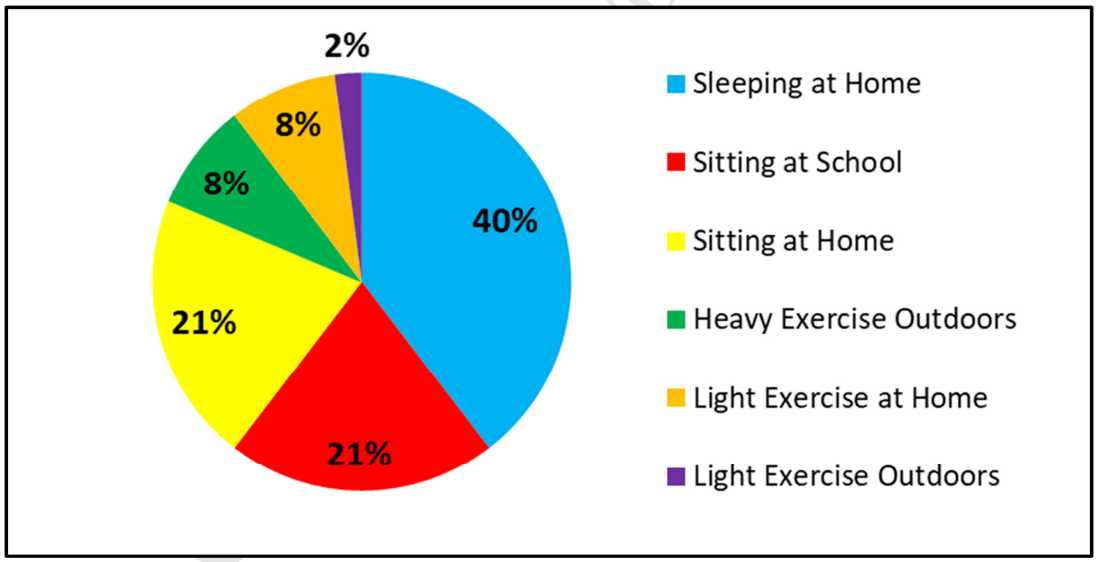

Figure 2

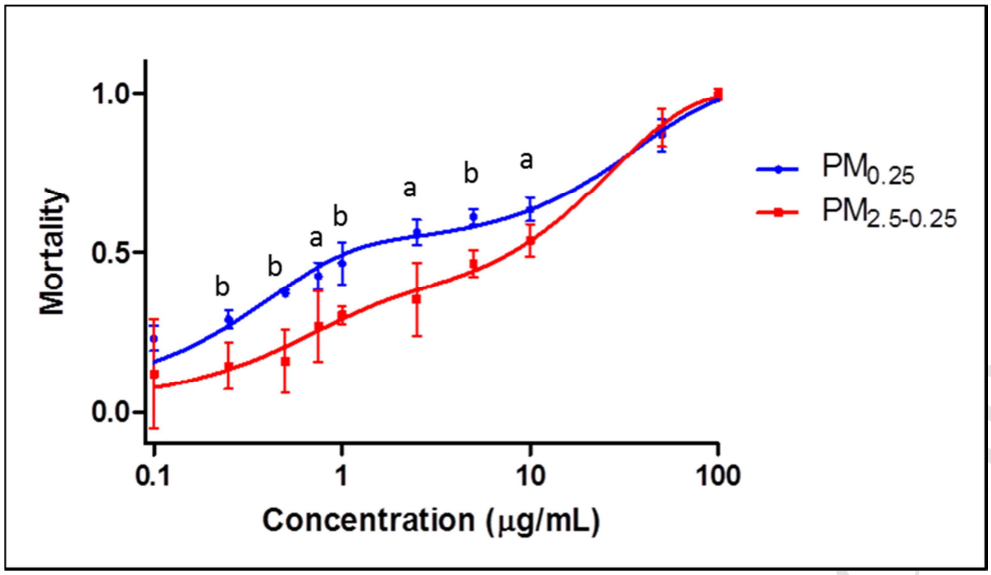

Figure 3

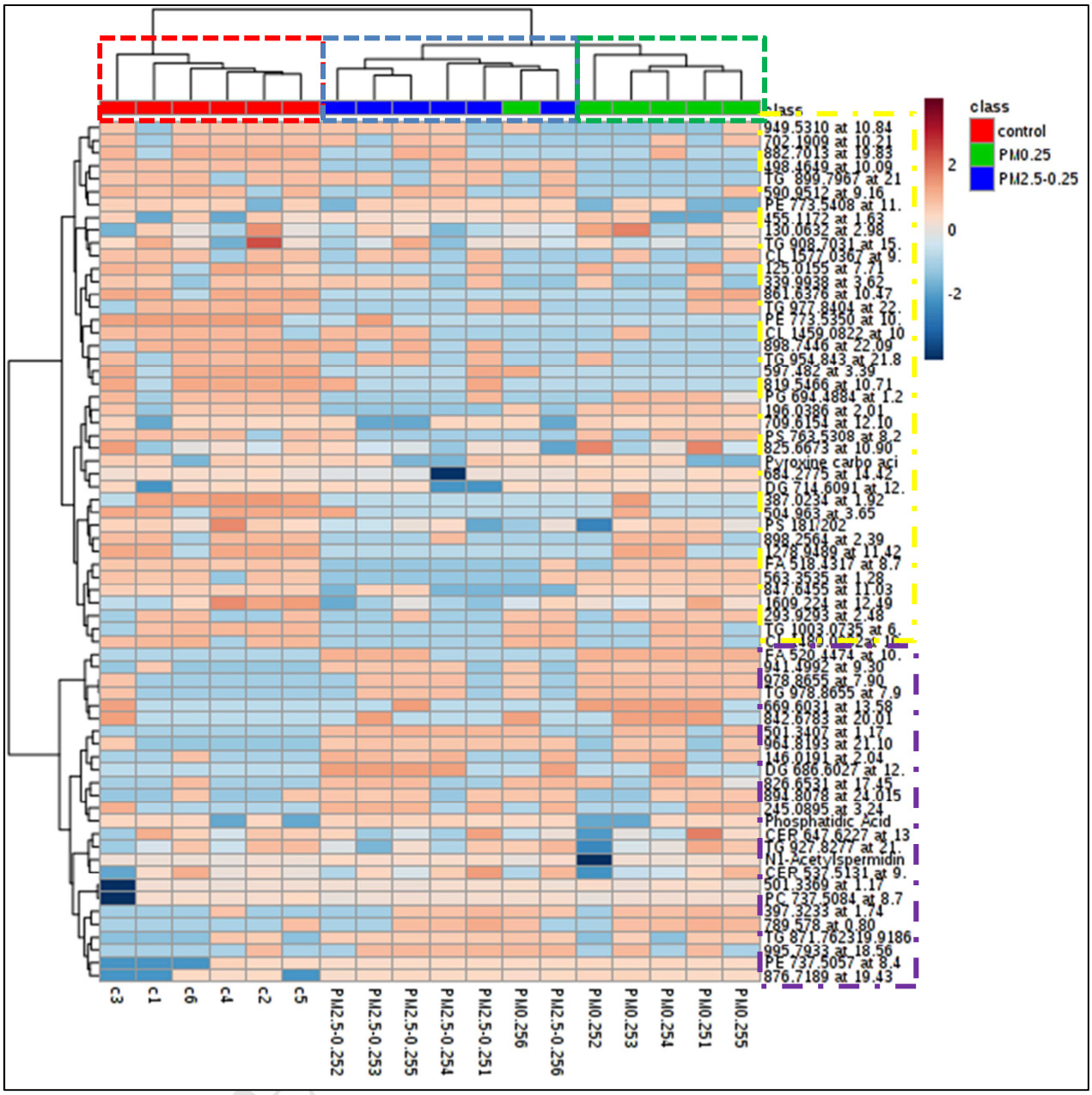

Figure 4

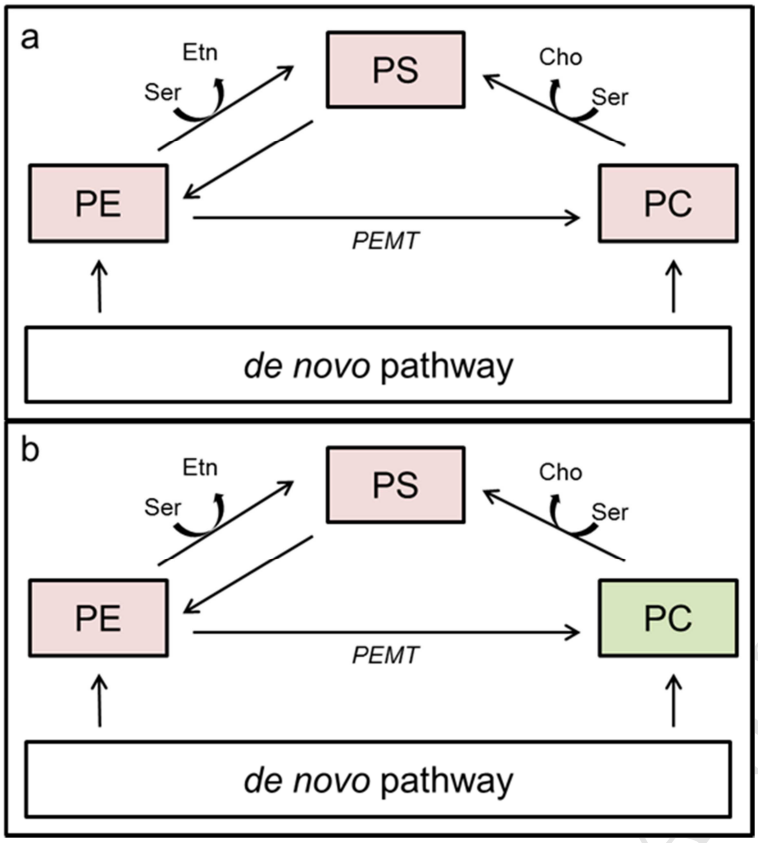

Figure 5

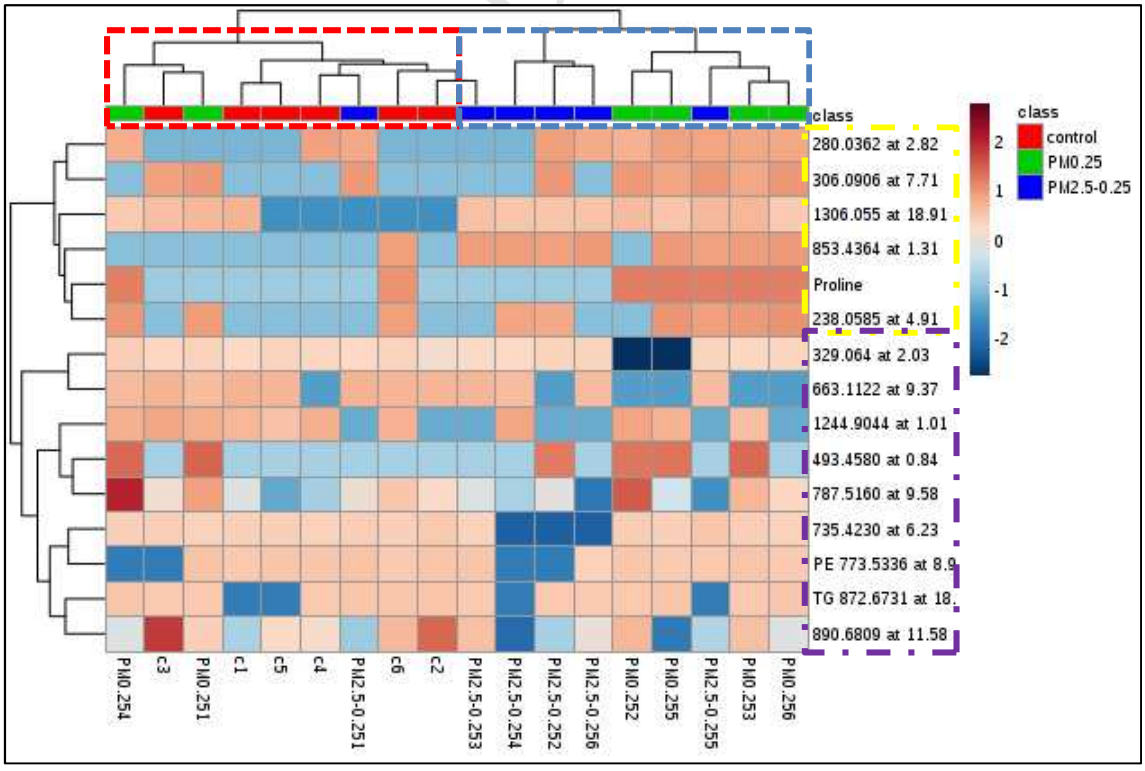

Figure 6

Highlights

- $PM_{10-2.5}$, $PM_{2.5-0.25}$, and $PM_{0.25}$ were sampled in indoor and outdoor environments.
- Toxicity and metabolism of A549 cells exposed to $PM_{2.5-0.25}$ and $PM_{0.25}$ were studied.
- $PM_{0.25}$ showed an overall higher toxicity than $PM_{2.5-0.25}$.
- $PM_{0.25}$ elicited a higher alteration in metabolism than $PM_{2.5-0.25}$.
- Most of the altered features were lipids present in cell and mitochondrial membranes.